JOURNAL OF PROPULSION AND POWER
Vol. 26, No. 4, July–August 2010

Theoretical Model of the Transient Combustion of Organic-Gellant-Based Gel Fuel Droplets

Alina Kunin,* Benveniste Natan,† and J. Barry Greenberg‡
Technion–Israel Institute of Technology, Haifa, Israel

DOI: 10.2514/1.41705

Experimental evidence of the combustion process of an all-organic gel fuel droplet indicates that at a certain time after ignition, evaporation of the liquid fuel results in the formation of an elastic layer of high-viscosity gellant around the droplet, which prevents further vaporization. As a result, constantly expanding vapor bubbles are produced within the droplet. Eventually, the layer ruptures and jets of fuel vapor are released. A theoretical, time-dependent model of organic-gellant-based gel droplet combustion has been developed and numerically solved. The results indicate that the evaporation rate of the liquid fuel from the droplet surface depends on droplet size and strongly affects the thickness of the gellant layer. The tensile stress, applied to the gellant layer during the formation of the bubbles, reaches high levels in short periods of time and causes the droplet to rupture when it exceeds the layer material rupture stress. The stage during which the gellant layer is formed is almost three orders of magnitude longer than the stage of bubble formation and layer rupture.

Nomenclature

c	=	mass concentration
D	=	diffusion coefficient
d	=	droplet diameter
H_{vap}	=	latent heat of vaporization
h_{gas}	=	heat transfer coefficient
k	=	mass transport coefficient of fuel gas from droplet to air
Mw	=	molecular weight
m	=	total mass of the droplet
$\dot{m}$	=	molar evaporation rate based on heat transfer
Nu	=	Nusselt number
p	=	pressure
p_f°	=	vapor pressure of fuel vapor
$p_{f,\text{surface}}$	=	fuel partial pressure adjacent to droplet surface
Q_{con}	=	heat transfer by convection
Q_{vap}	=	heat of vaporization
R_E	=	molar evaporation rate based on diffusion/kinetic limitations
r	=	radial coordinate
r_d	=	gel droplet radius
r_{TOT}	=	total gel droplet radius (second stage)
T	=	temperature
t	=	time
V_{TOT}	=	total volume of gel droplet (second stage)
$V_{\text{vapor-bubble}}$	=	volume of vapor bubble (second stage)
$\tilde{V}$	=	molar volume
X	=	gellant layer thickness

Greek Symbols

α	=	evaporation coefficient
γ	=	surface tension
λ_{gas}	=	air thermal conductivity
μ	=	viscosity
ν	=	Hertz–Knudsen impingement factor
ρ	=	density
σ	=	tensile stress
σ_{rup}	=	rupture stress
Ψ_{fg}	=	association parameter

Subscripts

amb	=	ambient conditions
BP	=	boiling point
f	=	liquid fuel
fg	=	liquid fuel/gellant mixture
g	=	gellant
0	=	initial conditions

Presented as Paper 2008-4871 at the 44th AIAA/ASEE/ASME/SAE Joint Propulsion Conference, Hartford, CT, 21–23 July 2008; received 21 Oct. 2008; revision received 28 Sept. 2009; accepted for publication 17 Dec. 2009.

*Graduate student, Faculty of Aerospace Engineering.
†Associate Professor, Faculty of Aerospace Engineering; Head, Missile Propulsion Laboratory. Associate Fellow AIAA.
‡Professor, Lady Davis Chair in Aerospace Engineering. Senior Member AIAA.

I. Introduction

THERE are two important parameters that have to be taken into account when considering the use of a propellant in various aerospace applications: energetic performance and safety features. Gel propellants are advantageous because they provide a promising response to both of these important requirements. In this particular liquid–solid state these unique propellants combine the advantages of liquid and solid propellants.

Gel fuels are liquid fuels whose rheological properties have been altered by the addition of gellants, so that they behave as non-Newtonian fluids. The existence of yield stress and increased viscosity can prevent agglomeration, aggregation, and separation of a metal solid phase from the fuel during storage. Consequently, these propellants are advantageous because of their capability to provide full energy management and because of their safety benefits over conventional liquid and solid propellants. Their performance characteristics and operational capabilities (which are similar to liquid propellants), as well as their high density, increased combustion energy, and long-term storage capability, make them attractive for many applications, especially for volume-limited propulsion system applications. An extensive review of various aspects of gel propellants was given by Natan and Rahimi [1].

In the present study we turn our attention to recent experimental work conducted by Solomon and Natan [2,3] on the combustion of organic-gellant-based fuels. They found that at the beginning of the burning process, an organic-gellant-based fuel droplet consists of a homogeneous, highly viscous liquid whose burning can be classified

as *classic* liquid droplet combustion with a distinct flame envelope that surrounds the droplet. In comparison to a liquid droplet, the turbulence intensity inside the droplet is low due to the high viscosity so that internal mixing is very slow. Because of the difference between the boiling-point temperature and the heat of vaporization of the liquid fuel and the organic gellant, the homogeneity of the mixture cannot be maintained and the concentration of the liquid fuel at the outer part of the droplet decreases continuously. At some point, a film of very high-viscosity gellant is formed around the droplet, enclosing the gel, and the result is that liquid fuel cannot pass through the gellant layer and evaporate towards the flame. Consequently, heating-up of the droplet results in the formation of fuel vapor bubbles inside the droplet. Expansion of the bubbles results in significant swelling of the droplet while the pressure inside the bubbles remains approximately constant. The thickness of the viscous gellant layer decreases as the droplet expands until the film is ruptured and jets of fuel vapor are released. The envelope collapses back onto the droplet and a new gellant layer is formed. This process repeats itself several times until the almost all-gellant residue droplet burns out completely. This behavior of a burning organic-gellant-based droplet is strikingly different from the behavior of burning pure liquid fuel droplets, which has been widely investigated both experimentally and theoretically during the last century.

In general, gel fuels consist of Z percent of gellant that can be organic or inorganic and (100-Z) percent of liquid fuel (mostly kerosene-based, e.g., JP-5 and JP-8 fuels). The gellant itself consists of a blend of components including a liquid solvent (e.g., methyl isoamyl ketone) and the actual gellant, which is an organic material. The advantage of organic gellants over inorganic ones is their ability to burn, whereas inorganic gellants are inert. Therefore, gel fuels can be regarded as multicomponent fuels with special and unique properties.

Extensive theoretical and experimental work has been conducted in the field of multicomponent fuel droplet evaporation/burning. Law [4] analyzed an isobaric, spherically symmetric combustion of a droplet whose temperature and composition are uniform within the droplet but are temporally varying (rapid mixing model). The theoretical results of Law indicated that vaporization is dominated by the most volatile species in the droplet and the droplet temperature is quite close to the steady-state boiling-point-temperature of that species. Sirignano [5] argued that the uniform temperature and concentration limit results from the infinite diffusivity limit, and the model should therefore be regarded as an infinite diffusivity model. In another theoretical work, Tong and Sirignano [6] proposed a different approach to the problem using a vortex model. This was basically a diffusion limit model that was previously formulated by Landis and Mills [7]. Based on these results, they concluded that the liquid-phase mass diffusion is extremely slow and represents the rate limiting process. By analyzing transient multicomponent droplet combustion Mawid and Aggarwal [8] found that the concentration of the fuel vapor inside the flame may become higher than that at the droplet surface and, as a result, suppression of the vaporization process may happen. These effects most likely occur due to high liquid-phase mass diffusion resistance, which prevents the more volatile component from diffusing rapidly to the droplet surface. Experimental work [9,10] confirmed most of the theoretical results mentioned above. However, all the aforementioned work was concerned with liquid fuel droplets.

Another field in which the chemical/physical processes resemble those that occur during gel fuel burning and which might provide important baselines and significantly contribute to the formulation of a gel fuel model is the field of metalized (slurry) droplets. A slurry fuel is a mixture of a liquid fuel and solid fuel, usually metal particles, that are sustained uniformly in the liquid medium. These metalized fuels have high energy-density potential; therefore, they can be advantageous mainly in air breathing propulsion systems. Antaki [11] presented the first theoretical model for the transient processes in the rigid slurry droplet during liquid vaporization and combustion. He assumed that after an initial period in which part of the liquid evaporates, a continuously thickening rigid porous shell is formed around the slurry droplet. During vaporization the outer radius remains constant while the surface of the inner sphere regresses with time due to liquid vaporization. He derived that motion of the regressing surface constitutes a d^3- law (the diameter of the inner sphere decreases cubically with time). Consequently, the porous-shell thickness increases as time goes by. Another fundamental study was conducted by Lee and Law [12]. They indicated that at the stage where the total volume is fixed by the shell, the continuous liquid gasification must create a continuously expanding vapor bubble in the interior of the slurry droplet; otherwise, the overall mass conservation is violated. Experimental results using carbon slurries were found to be in a good agreement with their theoretical model.

The aim of the present paper is to describe the peculiar phenomenon of the combustion process of a single organic-gellant-based gel fuel droplet in the framework of a theoretical time-dependent model. As a first step in establishing a physical model based upon the main mechanisms involved in the combustion of a gel droplet (as observed in experimental investigations), we implement an often-adopted strategy of an order-of-magnitude analysis. This enables us to carry out a straightforward mathematical/numerical analysis that leads to a relatively easy formulation of the problem and its solution. In the ensuing sections we explain the assumptions underlying the model; describe the model equations, boundary conditions, and method of solution; and in the final section discuss computed results that highlight the main characteristics of the organic-gellant-based gel fuel droplets combustion.

II. Problem Description and Mathematical Model

From the previously described experimental investigation on the combustion of an organic-gellant-based fuel droplet the most fundamental elements can be extracted: at a certain time, a film of high-viscosity gellant is created around the droplet, which prevents further evaporation of liquid fuel. Subsequently, a fuel vapor bubble is formed inside the droplet. The thickness of the viscous gellant layer decreases as the droplet expands until the film is ruptured, producing a jet of fuel vapor. The envelope collapses back into the droplet and a new layer is formed. The process of gel droplet burning is illustrated in Fig. 1.

Spherical symmetry is considered for the gel droplet combustion. The gel is treated as a bicomponent liquid mixture: liquid fuel and gellant. Although it is well-known that kerosene consists of various components of different boiling-point temperatures [13], at the current stage, the temperature within the droplet is assumed to be uniform and constant: the boiling-point temperature of the more volatile substance (liquid fuel). In reality, temperature changes with time as the droplet composition changes. However, experiments show that the temperature droplet change during the whole process is rather small (15%) [3]. In a single cycle (gellant layer formation, bubble creation, and layer rupture), the temperature change is insignificant; therefore, the assumption of constant temperature equal to the fuel boiling point is quite justified. For simplicity, it is assumed that the gel droplet has already been heated to the boiling-point temperature of the fuel and combustion takes place at ambient conditions, i.e., air at $T_{\text{amb}} = 2000$ K and $p_{\text{amb}} = 1$ atm. The viscosity of the gellant is significantly higher than that of the liquid fuel and at the current stage both of them are assumed constant, despite the fact that the gellant viscosity may decrease significantly during the heating process. By dividing the model into two stages, the physical/chemical mechanisms involved in the droplet during the burning process can be analyzed. During the first stage, fuel is consumed and an all-gellant layer is formed, as presented in Fig. 1a. The modification of the layer thickness with time occurs due to several factors such as liquid diffusion and vaporization through the layer. At the second stage, a bubble is formed and, as a result, the droplet expands and the layer thickness decreases until it ruptures (Fig. 1b) when the tensile stress reaches the layer rupture stress.

It is important to note that the mathematical formulation of the two stages concentrates mainly on internal droplet behavior. It is assumed that the flame surrounding the gel droplet produces a heat flux sufficient to vaporize the liquid fuel during the first stage and to enable formation of the vapor bubble in the droplet interior

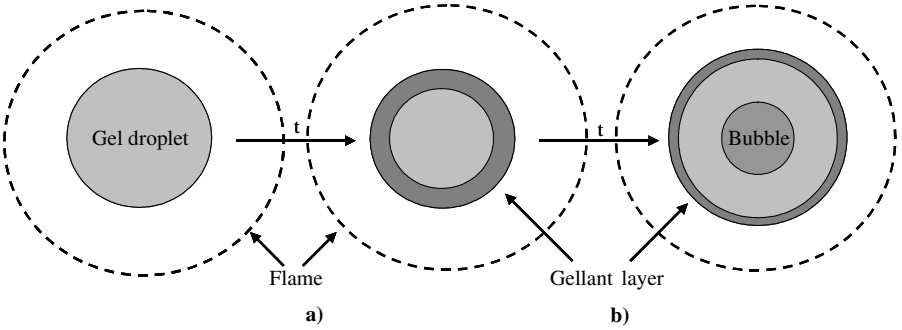

Fig. 1 Schematic of gel droplet burning.

during the second stage. In this way, the various processes occurring exterior to the droplet are not considered in the model development, and only what is happening inside the gel droplet is investigated. A more comprehensive model of the entire burning process including the interaction of gel droplet surface and flame is also possible at the expense of further complexity. This will be formulated in future work.

A. Model of the First Stage

The physical model of the first stage is described schematically in Fig. 1a. The actual reasons for the formation of the gellant layer are: a) the difference in the boiling points of the two components, the liquid fuel, and the gellant, and b) the absence of internal circulation, due to the relatively high viscosity of the mixture. Since the boiling point of the liquid fuel is significantly lower than that of the gellant, a monotonic decrease of the liquid fuel from the outer surface of the fuel droplet occurs as the combustion process begins. As a result, diffusion of the liquid fuel in the interior of the droplet occurs. The study by Saitoh and Nagano [14] also adopted this approach. The mass diffusivity coefficient of a binary liquid mixture strongly depends on temperature, pressure, and mixture composition. To estimate this coefficient, the empirical correlation proposed by Wilke [15] and by Wilke and Chang [16] is used:

$$D_{AB} = 7.4 \cdot 10^{-8} \frac{(\Psi_B M_B)^{1/2} T}{\mu \tilde{V}_A^{0.6}} \tag{1}$$

in which Ψ_B is the association parameter for the solvent B (recommended values for methanol, ethanol, and benzene are 1–1.9), M_B is the molecular weight, $\tilde{V}_A$ is the molar volume of the solute A, and T is temperature.

The empirical relation that Eyring and his coworkers [17] developed for the variation of viscosity with composition is described by

$$\log \mu_{fg}(t) = c_f(r,t) \log \mu_f + c_g(r,t) \log \mu_g \tag{2}$$

where $c_f(r,t)$ and $c_g(r,t)$ represent mass concentration of liquid fuel and gellant, respectively, along the droplet radius, and μ_f and μ_g represent viscosities of liquid fuel and gellant, respectively.

The last expression can be rewritten in the following, more convenient, way:

$$\mu_{fg}(t) = \mu_f^{c_f(r,t)} \mu_g^{c_g(r,t)} \tag{3}$$

so that the diffusion coefficient shown in Eq. (1) becomes

$$D_{fg} = 7.4 \cdot 10^{-8} \frac{(\Psi_{fg} \mathrm{Mw}_{fg})^{1/2} T_{\mathrm{BP}}}{\mu_{fg}(t) \tilde{V}_f^{0.6}} = \frac{\mathrm{Const}}{\mu_f^{c_f(r,t)} \mu_g^{c_g(r,t)}} \tag{4}$$

The general nonlinear, time-dependent diffusion equation in a spherically-symmetric coordinate system for a bicomponent mixture is

$$\frac{\partial c_f(r,t)}{\partial t} = \frac{1}{r^2} \frac{\partial}{\partial r} \left[D_{fg}(c_f(r,t)) r^2 \frac{\partial c_f(r,t)}{\partial r} \right] \tag{5}$$

In this equation, r represents the radial coordinate and t represents time. It is important to note that the last equation is valid for estimating the variation of both mass concentrations (liquid fuel and gellant) along the droplet radius, with time.

Two of the three initial and boundary conditions that are needed to solve the diffusion Eq. (5) presented above are

$$\begin{cases} t = 0: & c_f(r, t=0) = c_{f0} \ @ \ 0 \le r \le r_d \\ t > 0: & \frac{\partial c_f(r,t)}{\partial r} = 0 \ @ \ r = 0 \end{cases}$$

where r_d represents the gel droplet radius.

The third condition, concerning the mass concentration at the gel droplet surface, has to be formulated in order to provide a full solution to the diffusion equation; i.e., $c_f(t)@r = r_d$ for $t > 0$ is required.

The droplet radius r_d is assumed to be constant. The experimental results of [3] indicate that in the first stage the volume changes by approximately 5%, which means that the radius change is less than 2%, a fact that justifies the above assumption.

One of the strategies to tackle this problem is to consider the mass rate of evaporation from the droplet surface as a series of resistances, which include both the kinetic limitations on evaporation rate and the diffusion limitations on transport of gas to the air. Such a formulation was also adopted by King [18] in a different context:

$$\frac{R_E}{4\pi r_d^2} = \alpha \nu (p_f^\circ - p_{f,\mathrm{surface}}) = k(p_{f,\mathrm{surface}} - p_{f,\infty}) \tag{6}$$

where R_E represents the molar evaporation rate, ν represents the Hertz–Knudsen impingement factor, α represents the evaporation coefficient, k represents the mass transport coefficient for transport of fuel gas from the droplet to the air, p_f° represents the vapor pressure of fuel vapor, and $p_{f,\mathrm{surface}}$ represents the fuel partial pressure adjacent to droplet surface.

It is assumed that the partial pressure of liquid fuel far from the droplet is zero ($p_{f,\infty} = 0$).

By algebraic manipulation of Eq. (6), the following expression may be derived for R_E:

$$R_E = \frac{4\pi R^2 \alpha \nu p_f^\circ}{1 + \frac{\alpha \nu}{k}} \tag{7}$$

where ν and k are given by

$$\nu = \frac{1}{4R'' T} \sqrt{\frac{8R'T}{\pi (\mathrm{Mw})_f}} \tag{8}$$

$$k = \frac{D_{f,\mathrm{air}} Nu}{2R'' \cdot T \cdot r_d} \tag{9}$$

The gas law constants are $R' = 8.31447 \cdot 10^7 \ \frac{\mathrm{erg}}{\mathrm{mol\ K}}$ and $R'' = 82.0575 \ \frac{\mathrm{atm \cdot cm^3}}{\mathrm{mol\ K}}$; $D_{f,\mathrm{air}}$ represents the diffusivity of gaseous liquid

fuel in the air and Nu represents the Nusselt number (set equal to two). This comes from the assumption that the droplet is essentially stationary with respect to the surrounding gases.

A dimensionless group $\frac{k}{\alpha v}$ may be examined to determine the controlling process. If this parameter is near unity, the resistances of the evaporation and diffusion are nearly equal and neither resistance may be neglected. If it is much larger than unity, the process is essentially evaporation-rate-controlled, whereas for values much less than unity, the process is diffusion-controlled. In our case the evaporation coefficient is taken to be 10 (see the next section where this value is discussed).

Finally, the following expressions will serve as a third boundary condition for the diffusion equation at $r = r_d$:

$$\frac{\mathrm{d}m_f(t)}{\mathrm{d}t} = -R_E \cdot \mathrm{Mw}_f \tag{10}$$

$$m(t) = m_f(t) + m_g; \qquad c_f(r_d, t) = \frac{m_f(t)}{m(t)}; \qquad c_g(r_d, t) = \frac{m_g}{m(t)}$$

where $m(t)$ represents the total mass of the droplet, $m_f(t)$ represents the mass of liquid fuel, and $m_g(t)$ represents the mass of gellant:

$$t > 0\text{: } c_f(r_d, t) = \frac{m_f(t)}{m_f(t) + m_g} \tag{11}$$

Another straightforward way to estimate the molar evaporation rate from the droplet surface is to formulate the energy balance there. It is assumed that the ambient temperature is 2000 K (typical temperature in the combustion chamber) and, as was mentioned previously, the droplet temperature is stabilized at the boiling point of the liquid fuel. Consequently, the heat that is transferred by convection to the droplet surface will cause vaporization of liquid fuel.

Heat transfer by convection may be estimated from the following expression:

$$Q_{\mathrm{con}} = A \cdot h_{\mathrm{gas}} \cdot (T_{\mathrm{amb}} - T_{\mathrm{surface}}) \tag{12}$$

$$Nu = \frac{h_{\mathrm{gas}} d}{\lambda_{\mathrm{gas}}} \tag{13}$$

where λ_{gas} represents the air thermal conductivity at T_{amb}; $Nu = 2$, droplet at rest; $d = 2r_d$; and $T_{\mathrm{surface}} = T_{\mathrm{BP}}$.

Since $Q_{\mathrm{con}} = Q_{\mathrm{vap}}$, the fuel evaporation rate may be easily derived:

$$\dot{m} = H_{\mathrm{vap}}/Q_{\mathrm{vap}} \tag{14}$$

where H_{vap} represents the the latent heat of evaporation.

When the gellant concentration at the surface reaches 99%, liquid fuel cannot pass through the gel and this indicates the termination of the first stage. The actual estimation of the layer thickness is determined by the place where the composition of the gellant reaches at least 90%. The values of 99 and 90% are chosen arbitrarily. The results that are presented in the following sections indicate that these values are rather adequate.

B. Model of the Second Stage

The physical model of the second stage is described schematically in Fig. 1b. The formation of a gellant layer with a defined thickness characterizes the termination of the first stage. This gellant layer poses a barrier to the liquid fuel from penetrating through and evaporating towards the flame front. As a result, the formation of a vapor bubble in the interior of the droplet begins. Therefore, as the droplet expands, the layer thickness decreases until it ruptures when the tensile stress reaches the yield point of the material.

The total volume of the gel droplet $V_{\mathrm{TOT}}(t)$ consists of the volume of the vapor bubble $V_{\text{vapor-bubble}}(t)$ that is formed in the droplet interior and the remaining gellant + liquid fuel mixture volume $V_{fg}(t)$:

$$V_{\mathrm{TOT}}(t) = V_{\text{vapor-bubble}}(t) + V_{fg}(t) \tag{15}$$

$$V_{\text{vapor-bubble}}(t) = \frac{\dot{m}_{\text{vapor-bubble}} \cdot t}{\rho_{\text{vapor-bubble}}} \tag{16}$$

$$V_{fg}(t) = \frac{m_g}{\rho_g} + \frac{m_f(t)}{\rho_f} \tag{17}$$

where $\dot{m}_{\text{vapor-bubble}}$ represents the evaporation rate. Notice that at this stage no kinetic/diffusion resistance has to be taken into consideration; hence, $\dot{m}_{\text{vapor-bubble}} = \dot{m}$ and $\rho_{\text{vapor-bubble}}$ is the density of fuel gas.

Using $m_g(t) = m_g$ and $m_f(t) = m_{\text{stage}-2} - \dot{m}_{\text{vapor-bubble}} \cdot t$, the equation becomes

$$V_{\mathrm{TOT}}(t) = \frac{\dot{m}_{\text{vapor-bubble}} \cdot t}{\rho_{\text{vapor-bubble}}} \left(1 - \frac{\rho_{\text{vapor-bubble}}}{\rho_f}\right) + \frac{m_g}{\rho_g} + \frac{m_{\text{stage}-2}}{\rho_f}$$

To approximate the density ratio (fuel vapor to liquid fuel) the thermodynamic data of a typical fuel (octane) at 400 K and 1 atm were chosen:

$$\rho_{\text{vapor-bubble}} \approx 3.9 \ \frac{\mathrm{kg}}{\mathrm{m}^3}; \qquad \rho_f \approx 611 \ \frac{\mathrm{kg}}{\mathrm{m}^3}$$

Consequently, from this data it can be easily concluded that the change in the liquid interior volume is minor in comparison to the change in the vapor volume and it remains constant during the second stage:

$$V_{\mathrm{TOT}}(t) = \frac{\dot{m}_{\text{vapor-bubble}} \cdot t}{\rho_{\text{vapor-bubble}}} + V_{\mathrm{mixture}} \tag{18}$$

where $V_{\mathrm{mixture}} = \frac{m_g}{\rho_g} + \frac{m_{\text{stage}-2}}{\rho_f}$.

Based on these assumptions, as the total volume of the droplet increases during the second stage, the gellant layer thickness is given by

$$X(t) = \frac{r_d^2 X_0}{r_{\mathrm{TOT}}(t)^2} \tag{19}$$

where X_0 represents the initial layer thickness (estimated at the first stage).

The question that should be addressed at this point is, when does the organic-gellant layer rupture? To answer this question, the expression for the tensile stress applied to a thin spherical layer is described by

$$\sigma(t) = \frac{R(t) \cdot p}{2 \cdot X(t)} \tag{20}$$

Obviously, when the tensile stress reaches a certain value (rupture stress $\sim$ the yield point of the material), the gellant layer ruptures. In general, the rupture stress, similar to the yield stress, decreases with increasing temperature and decreasing gellant concentration: $\sigma_{\mathrm{rup}} = \sigma_{\mathrm{rup}}(c_g, T)$. Evaluation of the actual values of the rupture stress will be estimated experimentally in the near future. Meanwhile, in the present work, the development is completed by introducing a representative value of this parameter [19]. A typical rubber tensile stress, for example, is around 15 MPa (at room temperature), whereas the tensile stress of polyethylene (with low density) is around 4 MPa. As a first-order approximation, it is reasonable to assume that gellant rupture stress would also be of the same order of magnitude.

III. Solution

The solution domain is essentially divided into two stages. At the first stage, the formation of the gellant layer is obtained by solving the diffusion equation with appropriate initial and boundary conditions. This nonlinear parabolic equation is solved numerically using a

standard finite difference method. Satisfactory step sizes in the r and t directions were obtained by comparing computed results using a series of increasingly refined finite difference meshes to cover the region of the solution. Convergence of the numerical methods employed was checked in a standard fashion. The local accuracy of the method was of the order of the time step and the square of the radial increment. At the second stage, data from the first stage concerning the gellant layer thickness are substituted in appropriate expressions developed for the evaluation of this stage.

The following data are needed to evaluate various parameters developed in the proposed model and to obtain a rather simple but full theoretical solution to the model.

The droplet temperature is $T = 400$ K, whereas the ambient temperature is $T_{\text{amb}} = 2000$ K. The initial mass concentrations of the liquid fuel and of the gellant are $c_{f0} = 0.85$ and $c_{g0} = 0.15$, respectively.

Castor oil ($C_{57}H_{101}O_9$) and octane (C_8H_{18}) were chosen to represent the two components that comprise the gel fuel droplet, gellant, and conventional liquid fuel, respectively. Various properties of both of these components can be easily found in the literature. These properties are summarized below:

$$\text{Gellant: } \text{Mw}(C_{57}H_{101}O_9) = 929, \qquad \mu(C_{57}H_{101}O_9) = 800 \text{ cp}$$

$$\rho(C_{57}H_{101}O_9) = 1030 \ \frac{\text{kg}}{\text{m}^3}$$

$$\text{Liquid fuel: } \text{Mw}(C_8H_{18}) = 114.231, \qquad \mu(C_8H_{18}) = 0.2 \text{ cp}$$

$$\rho(C_8H_{18}) = 611 \ \frac{\text{kg}}{\text{m}^3}$$

The following correlations [20] were used to estimate viscosity, density, diffusivity in the air, vapor pressure, and latent heat of vaporization of octane: respectively:

$$\mu(C_8H_{18}) = 10^{\left(-5.9245+\frac{8.8809\cdot 10^2}{T}+1.2955\cdot 10^{-2}\cdot T-1.3596\cdot 10^{-5}\cdot T^2\right)} \text{ cp}$$

$$\rho(C_8H_{18}) = 0.22807 \cdot 0.25476^{-\left(1-\frac{T}{568.83}\right)^{0.2694}} \ \frac{\text{g}}{\text{ml}}$$

$$D_{C_8H_{18,\text{Air}}} = D_0\left(\frac{T_{\text{amb}}}{T_0}\right)^2\left(\frac{p_0}{p_{\text{amb}}}\right)$$

where

$$D_0(C_8H_{18,\text{Air}} \quad \text{at } T_0 = 273 \text{ K}; \qquad p_0 = 1 \text{ atm}) = 0.0505 \ \frac{\text{cm}^2}{\text{s}}$$

$$\log_{10} p^{\circ}_{C_8H_{18}} = A + \frac{B}{T} + C\log_{10} T + DT + ET^2; \quad p[\text{mmHg}], \quad T[\text{K}]$$

where

$$A = 29.0948; \qquad B = -3.0114E(3); \qquad C = -7.2653$$

$$D = -2.2696E(-11); \qquad E = 1.468E(-6)$$

$$H_{\text{vap}} = A \cdot \left(1 - \frac{T}{T_{\text{cr}}}\right)^n$$

where $A = 59.077$, $T_{\text{cr}} = 568.83$ K, and $n = 0.439$. For the case considered, $H_{\text{vap}} = 34.66 \ \frac{\text{kJ}}{\text{mole}}$.

In addition, the air thermal conductivity at 2000 K is $\lambda_g = 0.137 \ \frac{\text{W}}{\text{m K}}$ [21] and the rupture stress of the gallant (yield stress in tension) is assumed to be 2 MPa.

The dependence of the heat transferred by convection on droplet diameter is presented below:

Table 1 Dependence of the evaporation rates on droplet diameter

Diameter [μm]	R_E [$\frac{\text{mol}}{\text{s}}$] Based on kinetic/diffusion resistances	$\frac{k}{\alpha\nu}$	$\dot{m}$ [$\frac{\text{mol}}{\text{s}}$] Based on energy balance
50	$5.363 \cdot 10^{-7}$	0.0032	$1.988 \cdot 10^{-6}$
100	$1.074 \cdot 10^{-6}$	0.0016	$3.973 \cdot 10^{-6}$
200	$2.150 \cdot 10^{-6}$	0.0008	$7.946 \cdot 10^{-6}$

$$D = 50 \ \mu\text{m}: \ h_g = 5480 \ \frac{\text{W}}{\text{m}^2\text{K}}, \qquad Q_{\text{conv}} = 0.0689 \text{ W}$$

$$D = 100 \ \mu\text{m}: \ h_g = 2740 \ \frac{\text{W}}{\text{m}^2\text{K}}, \qquad Q_{\text{conv}} = 0.1377 \text{ W}$$

$$D = 200 \ \mu\text{m}: \ h_g = 1370 \ \frac{\text{W}}{\text{m}^2\text{K}}, \qquad Q_{\text{conv}} = 0.2754 \text{ W}$$

Now that all chemical parameters of both components comprising the gel fuel have been introduced we can turn to a discussion of the fuel evaporation rates developed in the previous section. The first (R_E) is calculated based on kinetic and diffusion resistance, whereas the second ($\dot{m}$) is based on an energy balance. For the following discussion the following droplet initial diameters will be considered: 50, 100, and 200 μm.

The final values of the evaporation rates (R_E and $\dot{m}$) together with dimensionless parameter $k/\alpha\nu$ appear in Table 1. It is seen that the dimensionless parameter is less than unity, which means that all processes are essentially diffusion-rate-controlled. In other words there is no limitation on evaporation, but there is a strong limitation on diffusion and this causes R_E to be less than $\dot{m}$. Nonetheless, all the heat transferred by convection is invested in evaporating the liquid fuel. As a result, as long as the evaporation process continues, the droplet temperature has to remain constant at the boiling point of the liquid fuel. Apparently, since $\dot{m}$ is a little higher than R_E, fuel vapor concentrates near the droplet surface without the ability to leave it and this slows down the decrease of liquid fuel concentration on the droplet surface. Admittedly, one can see some differences between the two coefficients, but considering the fact that they both rely on various empirical correlations, differences between them are more than acceptable. In any event, taking into account all these considerations, the actual evaporation rate will most likely lie between R_E and $\dot{m}$.

In Fig. 2, the dependence of the evaporation rate R_E on the evaporation coefficient α is presented. This monotonic function increases rapidly when $0 \le \alpha \le 1$ and then continues to increase asymptotically to $4\pi R^2 k p^{\circ}_{\text{fuel}}$ as $\alpha \to \infty$. In the present case, the evaporation coefficient is chosen to be 10.

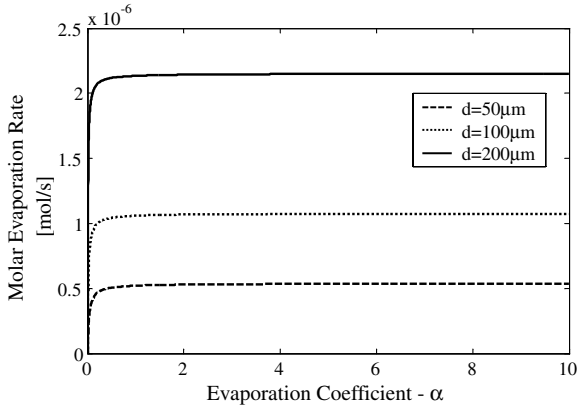

Fig. 2 Dependence of the molar evaporation rate R_E on the evaporation coefficient α.

IV. Results and Discussion

In the ensuing discussion, the numerical results obtained from both stages of the gel droplet combustion model are presented. Note that all the parameters appear in dimensional form.

The evolution of the mass concentrations of both components comprising the gel droplet, the liquid fuel, and the organic gellant in the interior of the droplet is presented in Figs. 3 and 4, for gel droplet diameters of 50 and 100 μm, respectively. In general, as expected, since the boiling point of the liquid fuel is lower than that of the gellant, the liquid fuel evaporates first, reducing its concentration, while the gellant concentration increases. In addition, for larger size droplets, the time that it takes to reach the same concentration also significantly increases; for example, to obtain $c_g > 0.99$ takes 0.25 ms for the first case compared with 4 ms for the second case.

In Fig. 5, the liquid fuel evaporation rate and its concentration on the droplet surface are shown. From this figure two main conclusions may be drawn. First, the evaporation rate and the time required for the fuel concentration at the surface to diminish to less than 1% increase as droplet diameter increases. As a result, the time it takes for the formulation of a gellant layer also increases. A second less straightforward but interesting conclusion concerns the actual gellant layer thickness. The droplet diameter has a significant influence on the thickness of the gellant layer; for high values of droplet diameter, the thickness of the gellant layer also increases. The last phenomenon can be easily explained. Considering the fact that the diffusion coefficient is very low (due to the enormous viscosity of the mixture), when the fuel concentration at the surface decreases rapidly (small diameter droplets), the layer, which is defined as the place where the gellant concentration attains more than 90%, is thinner in comparison to the case (large diameter droplets) in which the concentration decreases slowly providing minimal diffusion of the gellant and the fuel.

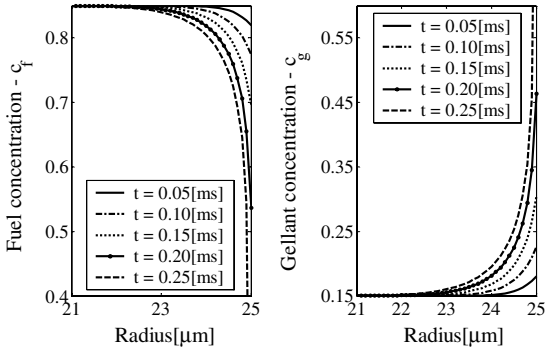

Fig. 3 Fuel and gellant concentrations in the droplet interior ($d = 50$ μm).

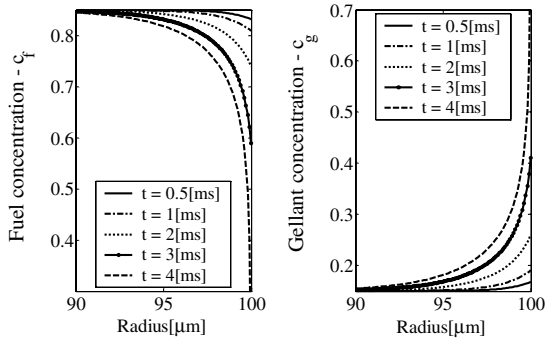

Fig. 4 Fuel and gellant concentrations in the droplet interior ($d = 100$ μm).

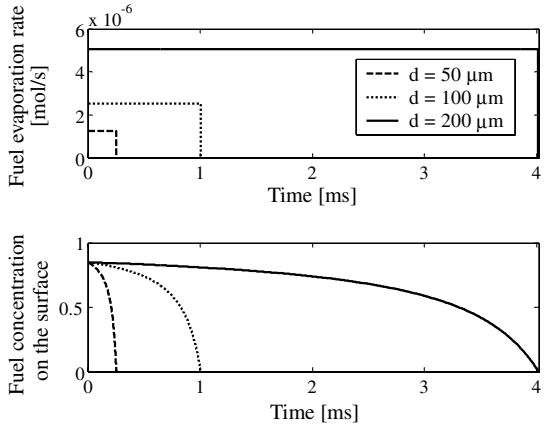

Fig. 5 Fuel evaporation rate and fuel concentration on the surface for initial droplet diameters of 50, 100, and 200 μm.

Table 2 Dependence of various parameters on the initial droplet diameter in the two stages of the model

	Stage I		Stage II	
Diameter (μm)	Initial gellant layer (nm)	Time (ms)	Final gellant layer (nm)	Time (μs)
50	55	0.25	19.2	0.42
100	64	1	30.7	0.86
200	76	4	51.3	1.38

The termination of the first stage is defined when the gellant concentration at the surface reaches 99%. At this point liquid fuel cannot penetrate through and evaporate towards the flame. As a result a constantly expanding vapor bubble in the droplet interior begins to evolve. The droplet expands and the layer thickness decreases until it ruptures when the tensile stress reaches the rupture stress of the material.

The most important results of both stages of the model are summarized in Table 2. It is shown that the first stage is significantly longer than the second, almost by three orders of magnitude. Furthermore, relatively small droplets ($d = 50$ μm) are capable of withstanding much higher pressure differences. As a result, their final gellant layer thickness is relatively small in comparison to larger droplets ($d = 200$ μm).

Figure 6a shows the development over time of the gellant layer thickness until rupture. The moment of the gellant layer rupture can be determined from Fig. 6b. When the tensile stress attains the rupture stress of the material, the second stage is terminated. The gellant layer ruptures and a jet of fuel vapor is released. In Figs. 7a and 7b, once again the normalized gellant layer thickness and the moment of the gellant layer rupture are presented but this time for a much larger droplet of $d = 100$ μm, in comparison to the previous figure, where a droplet of $d = 50$ μm is examined. The differences between the two cases are significant; the time until the gellant layer ruptures is almost twice as much for the large gel droplet (0.86 μs), whereas for the small droplet, it is only 0.42 μs. In addition, the final

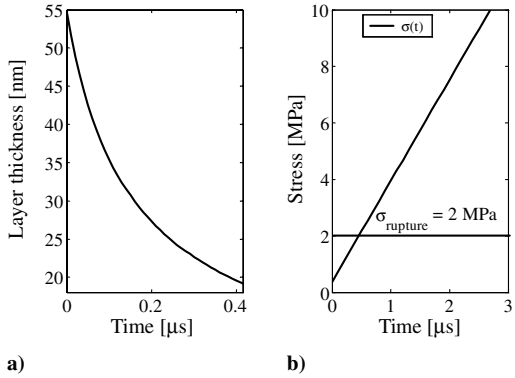

Fig. 6 a) Gellant layer thickness development with time and b) evolution of the tensile stress and the rupture stress as gellant layer thickness decreases ($d = 50$ μm).

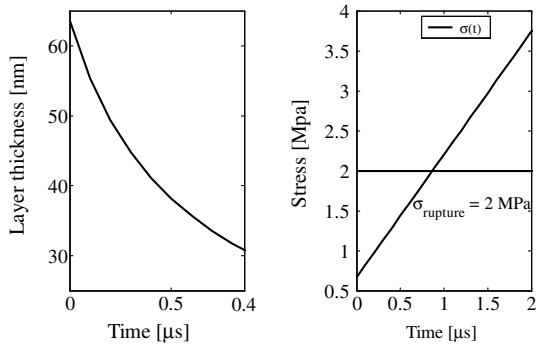

Fig. 7 a) Gellant layer thickness development with time and b) evolution of the tensile stress and the rupture stress as gellant layer thickness decreases ($d = 100$ μm).

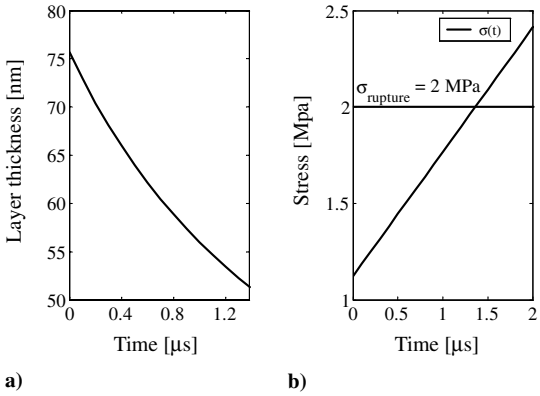

Fig. 8 a) Gellant layer thickness development with time and b) evolution of the tensile stress and the rupture stress as gellant layer thickness decreases ($d = 200$ μm).

thickness of the gellant layer at the moment of rupture is also different; for the large droplet it attains 30.7 nm, whereas for the small it is 19.2 nm. Figure 8a and 8b emphasize the two statements discussed earlier, but this time for a much larger droplet of $d=$ 200 μm. The moment of gellant layer rupture occurs after 1.38 μs, whereas the layer final thickness is 51.3 nm. These values are almost three times higher than the one obtained for a small droplet of $d = 50$ μm. Since smaller droplets are capable of withstanding much higher pressure differences, the final thickness of the gellant layer is thinner in comparison to large-size droplets.

V. Conclusions

The foundations of a theoretical model describing the phenomena involved in the combustion of organic-gellant-based gel droplets have been presented for the first time. According to the experimental investigation, during the burning of organic-gellant-based gels, an elastic layer made of gellant is formed around the droplet, which results in periodic swelling, bursting, and collapsing of the droplet. This burning process of gel droplets is totally different from the burning of pure liquid fuel droplets and repeats itself until all combustible material is consumed. The results demonstrated the profound importance of the droplet diameter on the magnitude of the gellant layer thickness; for large droplet diameter, the thickness of the layer also increases. Tensile stress, applied to the gellant film during the formation of the bubble in the droplet interior, reaches high magnitudes in a short period of time and causes the droplet to rupture as soon as it reaches the rupture stress of the layer material. The results show that the stage during which the gellant layer is formed is almost three orders of magnitude longer than the stage of bubble formation and the rupture of a droplet.

Acknowledgment

The authors express their gratitude to the Helen and Robert Asher Space Research Fund for the support of the present study.

References

[1] Natan, B., and Rahimi, S., "The Status of Gel Propellants in Year 2000," *Combustion of Energetic Materials*, edited by K. K. Kuo and L. DeLuca, Begell House, New York, 2002, pp. 172–194.

[2] Solomon, Y., and Natan, B., "Experimental Investigation of the Organic Gellant-Based Gel Fuel Droplets," *Combustion Science and Technology*, Vol. 178, No. 6, June 2006, pp. 1185–1199. doi:10.1080/00102200600620259

[3] Solomon, Y., Natan, B., and Cohen, Y., "Combustion of Gel Fuels Based on Organic Gellants," *Combustion and Flame*, Vol. 156, No. 1, 2009, pp. 261–268. doi:10.1016/j.combustflame.2008.08.008

[4] Law, C. K., "Multicomponent Droplet Combustion with Rapid Internal Mixing," *Combustion and Flame*, Vol. 26, No. 2, 1976, pp. 219–233. doi:10.1016/0010-2180(76)90073-0

[5] Sirignano, W. A., "Theory of Multi-Component Fuel Droplet Vaporization," *Archives of Thermodynamics and Combustion*, Vol. 9, No. 2, 1978, pp. 231–247.

[6] Tong, A. Y., and Sirignano, W. A., "Multi-Component Droplet Vaporization in a High Temperature Gas," *Combustion and Flame*, Vol. 66, No. 3, 1986, pp. 221–235. doi:10.1016/0010-2180(86)90136-7

[7] Landis, R. B., and Mills, A. F., "Effect of Internal Diffusional Resistance on the Evaporation of Binary Droplets," *Proceedings of the 5th International Heat Transfer Conference*, Society of Heat Transfer of Japan, Tokyo, Japan, 1974, pp. 345–349.

[8] Mawid, M., and Aggarwal, S. K., "Analysis of Transient Combustion of a Multicomponent Liquid Fuel Droplet," *Combustion and Flame*, Vol. 84, No. 2, 1991, pp. 197–209. doi:10.1016/0010-2180(91)90048-G

[9] Wang, C. H., Liu, X. Q., and Law, C. K., "Combustion and Microexplosion of Freely Falling Multicomponent Droplets," *Combustion and Flame*, Vol. 56, No. 2, 1984, pp. 175–197. doi:10.1016/0010-2180(84)90036-1

[10] Wang, C. H., and Law, C. K., "Microexplosion of Fuel Droplets under High Pressure," *Combustion and Flame*, Vol. 59, No. 1, 1985, pp. 53–62. doi:10.1016/0010-2180(85)90057-4

[11] Antaki, P., "Transient Processes in a Rigid Slurry Droplet During Liquid Vaporization and Combustion," *Combustion Science and Technology*, Vol. 46, No. 3, 1986, pp. 113–135. doi:10.1080/00102208608959796

[12] Lee, A., and Law, C. K., "Gasification and Shell Characteristics in Slurry Droplet Burning," *Combustion and Flame*, Vol. 85, No. 1, 1991, pp. 77–93. doi:10.1016/0010-2180(91)90178-E

[13] Edwards, T., "Kerosene Fuels for Aerospace Propulsion," AIAA Paper 2002-3874, July 2002.

[14] Saitoh, T., and Nagano, O., "Transient Combustion of a Fuel Droplet with Finite Rate of Chemical Reaction," *Combustion Science and Technology*, Vol. 22, No. 5, 1980, pp. 227–234. doi:10.1080/00102208008952386

[15] Wilke, C. R., "Estimation of Liquid Diffusion Coefficients," *Chemical Engineering Progress*, Vol. 45, 1949, pp. 218–224.

[16] Wilke, C. R., and Chang, P. C. "Correlation of Diffusion Coefficients in Dilute Solutions," *American Institute of Chemical Engineers Journal*, Vol. 1, No. 2, 1955, pp. 264–270.

[17] Glasstone, S., Laidler, K. J., and Eyring, H., *Theory of Rate Processes*, McGraw–Hill, New York, 1941.

[18] King, M. K., "Boron Particle Ignition in Hot Gas Streams," *Combustion Science and Technology*, Vol. 8, No. 6, 1973, pp. 255–273. doi:10.1080/00102207308946648

[19] Al-Sammerrai, D., and Al-Nidawy, N. K., "Polyethylene: Synthesis, Properties and Uses," *Handbook of Polymer Science and Technology-Performance, Vol. 2: Properties of Plastics and Elastometers*, edited by Cheremisinoff, N. P., Marcel Dekker, New York, 1989, pp. 341–366.

[20] Yaws, C. L., *Chemical Properties Handbook*, McGraw–Hill, New York, 1999.

[21] Perry, R. H., and Green, D. W., *Perry's Chemical Engineers Handbook*, 7th ed., McGraw–Hill, New York, 1997.

C. Avedisian
Associate Editor